VEGF and TGF-β are required for the maintenance of the choroid plexus and ependyma

Arindel S.R. Maharaj,[3,4] Tony E. Walshe,[3,4] Magali Saint-Geniez,[3,4] Shivalingappa Venkatesha,[4,5] Angel E. Maldonado,[3,4] Nathan C. Himes,[4] Kabir S. Matharu,[3] S. Ananth Karumanchi,[4,5] and Patricia A. D'Amore[1,2,3,4]

[1]Department of Ophthalmology, [2]Department of Pathology, and [3]Schepens Eye Research Institute, [4]Harvard Medical School, Boston, MA 02114
[5]Beth Israel Deaconess Medical Center, Boston, MA 02215

Although the role of vascular endothelial growth factor (VEGF) in developmental and pathological angiogenesis is well established, its function in the adult is less clear. Similarly, although transforming growth factor (TGF) β is involved in angiogenesis, presumably by mediating capillary (endothelial cell [EC]) stability, its involvement in quiescent vasculature is virtually uninvestigated. Given the neurological findings in patients treated with VEGF-neutralizing therapy (bevacizumab) and in patients with severe preeclampsia, which is mediated by soluble VEGF receptor 1/soluble Fms-like tyrosine kinase receptor 1 and soluble endoglin, a TGF-β signaling inhibitor, we investigated the roles of VEGF and TGF-β in choroid plexus (CP) integrity and function in adult mice. Receptors for VEGF and TGF-β were detected in adult CP, as well as on ependymal cells. Inhibition of VEGF led to decreased CP vascular perfusion, which was associated with fibrin deposition. Simultaneous blockade of VEGF and TGF-β resulted in the loss of fenestrae on CP vasculature and thickening of the otherwise attenuated capillary endothelium, as well as the disappearance of ependymal cell microvilli and the development of periventricular edema. These results provide compelling evidence that both VEGF and TGF-β are involved in the regulation of EC stability, ependymal cell function, and periventricular permeability.

CORRESPONDENCE
Patricia A. D'Amore:
patricia.damore@
schepens.harvard.edu

Abbreviations used: Ad, adenovirus; CNS, central nervous system; coll IV, type IV collagen; CP, choroid plexus; CSF, cerebrospinal fluid; EC, endothelial cell; Gd, gadopentetate dimeglumine; H + E, hematoxylin and eosin; MRI, magnetic resonance imaging; RPLS, reversible posterior leukoencephalopathy syndrome; sEng, soluble endoglin; sFlt1, soluble Fms-like tyrosine kinase receptor 1; TEM, transmission electron microscopy; VEGF, vascular endothelial growth factor; VP, viral particles.

Vascular endothelial growth factor (VEGF; vascular permeability factor) is required during embryogenesis for vasculogenesis, the de novo formation of blood vessels from hemangioblasts, and for angiogenesis, the formation of new vessels from existing vessels (1). Moreover, vascular development is dependent on tight regulation of VEGF, as mice lacking a single *VEGF* allele die by embryonic day 8.5 with severe vascular defects (2, 3). Similarly, overexpression of *VEGF* results in embryonic lethality (4). In the adult, VEGF is required for physiological angiogenesis, including tissue repair (5) and female reproduction (6). It also mediates vessel proliferation in many pathologies, including age-related macular degeneration, diabetic retinopathy, and cancer (7, 8).

In vitro studies have shown that VEGF is required for endothelial cell (EC) survival (9) and can mediate the formation of fenestrations (10). Furthermore, in vivo analysis points to a role for VEGF in the maintenance of a fenestrated EC phenotype (11, 12). Consistent with this, VEGF is expressed by the retinal pigmented epithelium adjacent to the choriocapillaris (13), by podocytes bordering the glomerular endothelium, and by choroid plexus (CP) epithelium abutting the CP microvasculature (14). In addition to the emerging function for VEGF in mature ECs, in vitro and in vivo studies indicate that VEGF also acts on several nonvascular cells, including immune cells and neural cells (for reviews see references 15, 16).

Given the role of VEGF in tumor growth and metastasis, drugs targeting VEGF have become part of many antitumor therapies. Although the first FDA-approved anti-VEGF agent, bevacizumab (Avastin; Genentech), improves survival in patients with metastatic colorectal cancer and small cell lung carcinoma,

A.S.R. Maharaj and T.E. Walshe contributed equally to this work.

consistent side effects include hypertension, proteinuria, and thrombosis, indicating that systemic VEGF blockade leads to vascular and tissue dysfunction (17–19).

Similar conclusions come from observations of preeclampsia. Preeclampsia (for review see reference 20), a disease of pregnancy that affects 4–5% of women beginning in the second trimester, is mediated by elevated levels of placenta-derived factors that lead to systemic endothelial dysfunction, with symptoms including hypertension and proteinuria. Among the factors overexpressed in preeclampsia is soluble VEGFR1/soluble Fms-like tyrosine kinase receptor 1 (sFlt1), an endogenous VEGF inhibitor. The administration of sFlt1 to pregnant rats leads to hypertension, proteinuria, thrombosis, and glomerular injury (21), all of which are observed in both preeclampsia and in patients treated with bevacizumab (22).

Untreated, preeclampsia may progress to eclampsia, which is marked by severe central nervous system (CNS) symptoms, including headaches, altered mental status, blurred vision, blindness, seizures, and stroke. Brain magnetic resonance imaging (MRI) of severely preeclamptic women reveal lesions characteristic of reversible posterior leukoencephalopathy syndrome (RPLS) (23). Interestingly, RPLS has also been reported in bevacizumab-treated patients (24, 25). RPLS is associated with several vascular disorders, including eclampsia, thrombotic thrombocytopenic purpura, and cyclosporine toxicity, and it is believed that a primary insult to the endothelium may underlie the neurological findings. The notion that VEGF neutralization might directly affect the brain is supported by observations of VEGF expression in the adult brain, with particularly high expression in the CP (14).

VEGF expression is regulated by a variety of growth factors, including TGF-β (26). Contact between ECs and mural cells in vitro leads to the local activation of latent TGF-β, which acts on ECs and pericytes, causing a wide range of effects, including the inhibition of endothelial proliferation and migration (27, 28), induction of mural cell differentiation, and pericyte production of VEGF (9). TGF-β also stimulates VEGF production by several other cell types, including epithelial cells (29), macrophages (30), and osteoblasts (31).

Soluble endoglin (sEng), a circulating TGF-β signaling inhibitor, is also elevated in the serum of preeclamptic patients (32, 33). sEng, the proteolytically cleaved extracellular domain of the TGF-β coreceptor Eng (CD105), can neutralize free TGF-β1 and TGF-β3. Coexpression of sEng and sFlt1 in pregnant rats increases the severity of the phenotype (as compared with sFlt1), including hypertension, proteinuria, permeability, thrombocytopenia, and liver and kidney damage, all of which are associated with severe preeclampsia (20).

Based on our previous observations of VEGF expression in the CP (14), as well as clinical findings of CNS symptoms, including RPLS in preeclamptic/eclamptic patients, we hypothesized that VEGF and TGF-β are required for the stability and maintenance of the CP and that blockade of these molecules would result in CNS damage. We report the effects of VEGF and TGF-β neutralization in the CP and ependyma of adult mice.

RESULTS

VEGF, TGF-β1, and their receptors in adult mouse CP and ependyma

A prerequisite for VEGF and/or TGF-β to play a role in maintenance of the CP is the expression of both the receptor and ligand. Given that VEGF is robustly expressed in the CP epithelium (14) and that TGF-β1 has been immunolocalized in the CP (34), we sought to determine the expression of VEGFR2, TGF-β1, and TGF-βR2 in the CP. RT-PCR of CP dissected from adult mice revealed the expression of VEGFR2 and TGF-βR2, as well as TGF-β1 (Fig. 1 A). Analysis of VEGF isoforms by real-time RT-PCR showed *VEGF120*, which is freely diffusible, as the predominant isoform (52.6%), followed by *VEGF164* (45.6%), and very low levels (1.7%) of *VEGF188* (Fig. 1 B). The high proportion of the soluble form of VEGF motivated us to examine the localization of VEGFR2, the primary signaling receptor of VEGF. Immunohistochemistry of *VEGF-lacZ* mouse brain sections revealed VEGFR2 expression in the CP vasculature (Fig. 1 C, black arrows) underlying the VEGF-expressing CP epithelium (arrowheads). Unexpectedly, we also found VEGFR2 to be expressed by ependymal cells lining the ventricles (Fig. 1 C, red arrows). Immunohistochemistry also revealed TGF-βR2 on CP epithelial cells and ependymal cells (Fig. 1 D, arrows and arrowheads, respectively). The presence of both ligands and receptors for VEGF and TGF-β is consistent with a role for these factors in CP and ependymal cells.

Neutralization of VEGF or VEGF and TGF-β results in CP vasculature and ependymal cell defects

To determine the function of VEGF and TGF-β in the CP, we injected adult mice intravenously with adenovirus (Ad)-sFlt1 or Ad-sEng, a combination of Ad-sFlt1 + Ad-sEng, or Ad-null using previously described Ad constructs and titers (32). Plasma sFlt1 and sEng levels of ∼200 ng/ml were determined by ELISA 7 d after injection and were sustained for at least 21 d for sFlt1 and 14 d for sEng (unpublished data).

To determine the effects of neutralizing VEGF and/or TGF-β on CP vascular blood flow, mice were perfused with high mol wt FITC-dextran after 14 d of infection. Immunostaining of brain sections for type IV collagen (coll IV; Fig. 2 A), which as a component of the vascular basement membrane outlines all blood vessels (35), revealed 95.2% ($n = 5$) colocalization with FITC-dextran in Ad-null–expressing mice (Fig. 2, A and B). Perfusion of the CP vasculature was not significantly altered by the expression of Ad-sEng (92%; P = NS; $n = 6$; Fig. 2 B). There was a significant decrease in the perfusion of the CP vessels in mice expressing sFlt1 (73.3%; $P < 0.02$; $n = 6$; Fig. 2 B) and in mice expressing sFlt1 + sEng (72.6%; $P < 0.001$; $n = 6$; Fig. 2 B). Hematoxylin and eosin (H + E) staining (Fig. 2 C) and immunohistochemical localization of fibrinogen, as a surrogate for fibrin deposition as previously described (Fig. 2 D) (36), in serial sections revealed multiple thrombi in Ad-sFlt1 and Ad-sFlt1 + Ad-sEng mice (arrows) but not in Ad-null– or Ad-sEng–expressing mice.

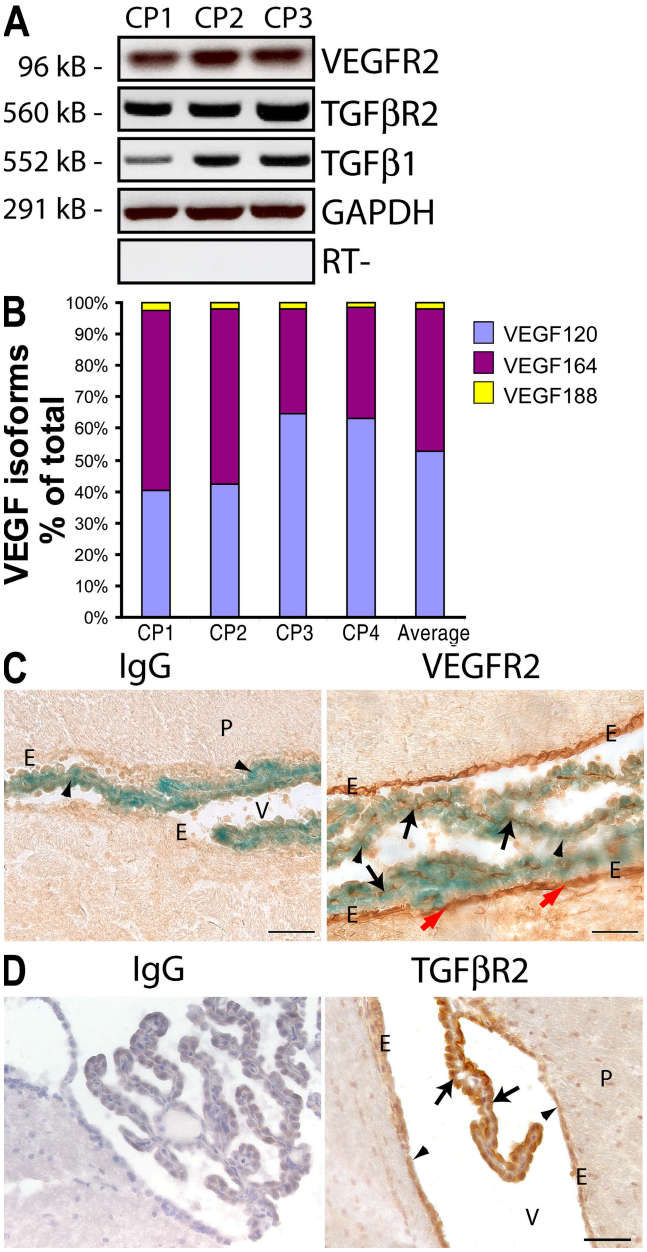

Figure 1. Expression of VEGF, TGF-β1, VEGFR2, and TGF-βR2 in the CP and ependyma. (A) RT-PCR of complementary DNA from CP dissected from the lateral third and fourth ventricles of four adult mice (n = 3 pools) revealed expression of TGF-β1 and its receptor, TGF-βR2, as well as VEGFR2. (B) Real-time RT-PCR of CP complementary DNA (n = 4 pools) for VEGF isoforms (52.6% *VEGF120*, 45.5% *VEGF164*, and 1.8% *VEGF 188*). (C) Staining of *VEGF-lacZ* brain sections for *lacZ* (blue) and AEC immunostaining for VEGFR2 (red) revealed VEGFR2 in the CP vasculature (black arrows) adjacent to VEGF-expressing CP epithelial cells (arrowheads) and in the ependymal lining of the ventricle (red arrows). (D) DAB immunostaining followed by hematoxylin staining of adult brain sections for TGF-βR2 reveals TGF-βR2 immunoreactivity in the CP epithelia (arrows) and ependyma (arrowheads). E, ependyma; P, parenchyma; V, ventricle. Bars, 50 μm.

Apoptosis is tightly regulated through several gene products, including members of the Bcl-2 family of genes in the CP (37). We examined the relative levels of messenger RNA for the *Bcl-2* family in the CP. When compared with Ad-null, the CP from both Ad-sEng– and Ad-sFlt1–expressing mice expressed significantly less antiapoptotic *Bcl-x_L* (0.64 ± 0.11 and 0.74 ± 0.04, respectively; $P < 0.05$; $n = 4$), whereas Ad-sFlt1 + Ad-sEng had significantly less antiapoptotic *Bcl-x_L* and *bcl-2* (0.4 ± 0.13 and 0.58 ± 0.09, respectively; $P < 0.05$; $n = 4$; Fig. 2 E). No change in proapoptotic *bax* or *bad* gene expression was detected in any of the groups.

Transmission electron microscopy (TEM) of the fenestrations in CP vasculature revealed near complete loss of endothelial fenestrae and swelling of the ECs of mice expressing sFlt1 + sEng but no significant change in mice expressing Ad-null, Ad-sFlt1, or Ad-sEng (Fig. 3, A and B). Ultrastructural analysis revealed the loss of microvilli on ependymal cells in mice expressing Ad-sFlt1 + Ad-sEng for 14 d (Fig. 3 C, arrows) but not in mice expressing Ad-null, Ad-sFlt1, or Ad-sEng for 14 d. Although microvilli were absent from mice expressing sFlt1 + sEng, the mitochondrial localization and nuclei of the ependymal cells appeared relatively normal (Fig. 3 C). Collectively, the results of the perfusion analysis and ultrastructural features indicate that VEGF and TGF-β are required for stability of the CP endothelium and for maintaining the integrity of the ependymal lining of the ventricle.

Neutralization of VEGF and TGF-β results in cortical periventricular focal lesions

Focal contrast enhancement associated with leukoencephalopathy is observed in preeclamptic patients who progress to eclampsia, as well as in some patients treated with bevacizumab (23–25), and arises from barrier dysfunction and local changes in permeability. Based on TEM findings, we hypothesized that the decreased vascular perfusion and loss of ependymal cell microvilli observed with the inhibition of VEGF and TGF-β might compromise the ventricular function. To test this, we measured extravasated Evans blue in mice after 3 d of Ad infection. Mice expressing sFlt1 + sEng, but none of the other groups, showed a significant increase in Evans blue extravasation (OD_{620nm} = 0.218 ± 0.09 vs. 0.045 ± 0.044 for Ad-null; $P < 0.05$; n = 3 and 4, respectively; Fig. 4 A).

H + E–stained sections of the lateral ventricles revealed periventricular edema in mice expressing sFlt1 + sEng at 14 d (arrows) but not in other experimental groups (Fig. 4 B). To more precisely define the extent of increased permeability, experimental mice were subjected to MRI with gadopentetate dimeglumine (Gd) contrast after 8 and 16 d of infection. Gd does not cross the intact blood–brain barrier and, thus, is a direct marker for blood–brain barrier disruption (38). In this study, a high dose of Gd (0.3 mM/kg body wt) was used to maximize detection. T1-weighted MRI on mice infected for 8 (Fig. 4 C) or 16 (Fig. 4 D) d revealed lesions surrounding the lateral ventricle in the midbrain in animals expressing sFlt1 and sEng but not in other groups. Quantification of the periventricular lesion signal intensity revealed a significant increase

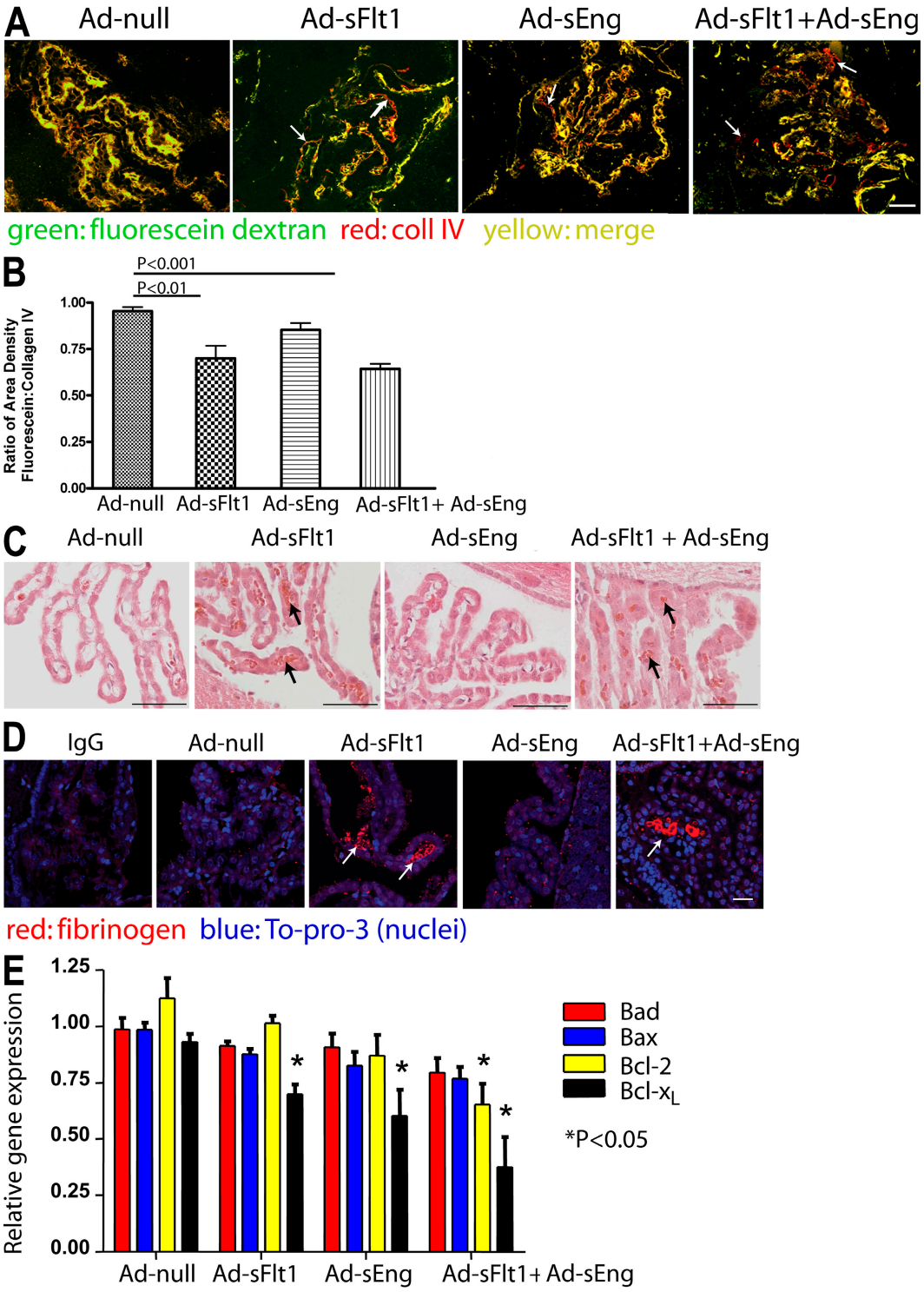

Figure 2. VEGF neutralization results in decreased CP vascular perfusion and fibrin deposition. (A) Mice perfused with high mol wt fluorescein dextran show a significant decrease in vessel perfusion in Ad-sFlt1 as well as in Ad-sFlt1 + Ad-sEng mice (arrows). Nonperfused vessels are identified as coll IV positive (red) and fluorescein negative. (B) Perfused blood vessels were quantified by measuring the proportion of sectional area occupied by fluorescein (green) and coll IV fluorescence (red; adapted from reference 63). Results represent the mean value of three sections 150 μm apart per mouse, and the mean of five to six animals. (C) H + E staining (black arrows) and (D) immunofluorescent staining (white arrows) for fibrinogen in CP show multiple fibrin clots in Ad-sFlt1 (C and D, arrows) and Ad-sFlt1 + Ad-sEng (C and D). (E) Relative messenger RNA expression of proapoptotic (*bad* and *bax*) and antiapoptotic (*Bcl-2* and *Bcl-x*$_L$) genes in CP were determined by real-time PCR analysis. Bars: (A and C): 50 μm; (D) 25 μm.

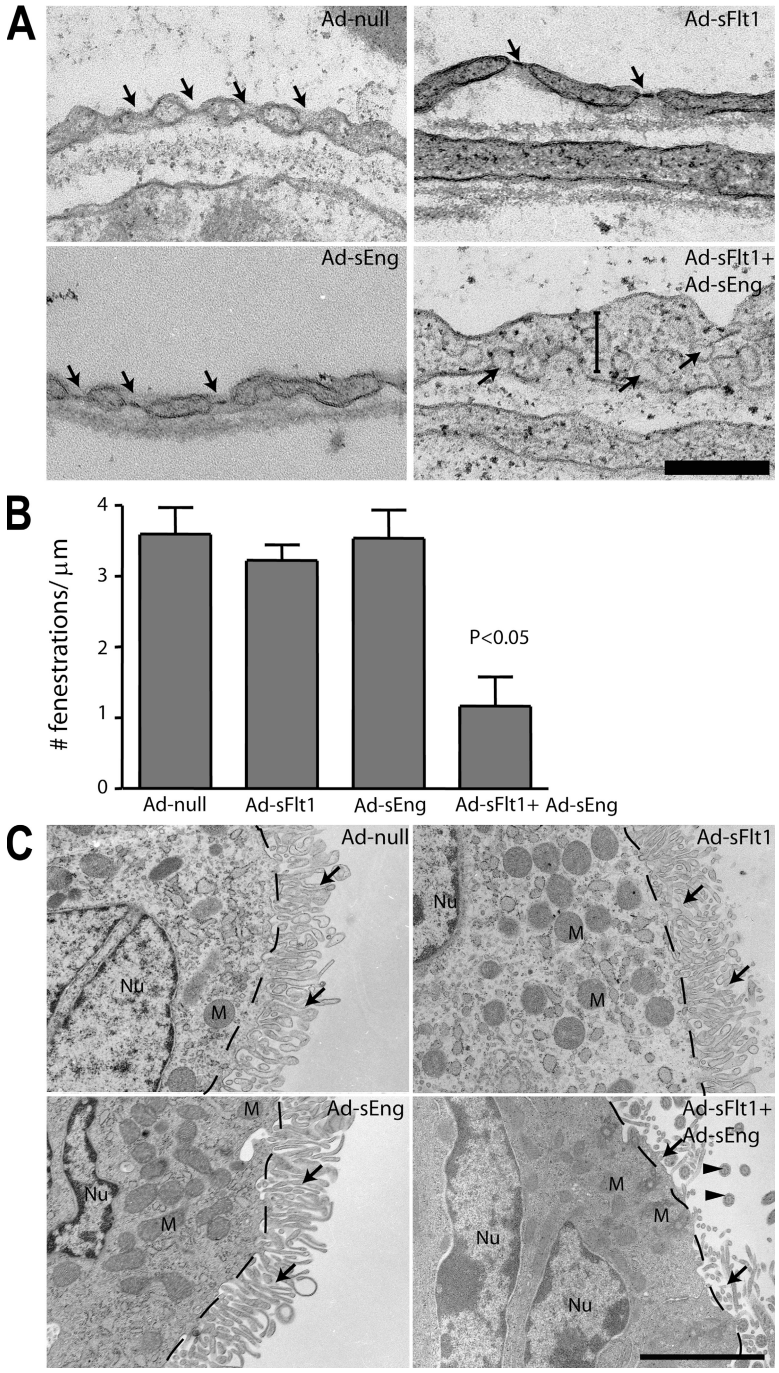

Figure 3. Effect of VEGF and TGF-β neutralization on the ultrastructure of CP vasculature and the ependyma. After 14 d of infection with the indicated Ad's, the CP and ependyma were examined by TEM. (A) In the CP vasculature, fenestrations (arrows) were unaffected in Ad-null, Ad-sFlt1, and Ad-sEng mice, whereas mice expressing Ad-sFlt1 + Ad-sEng exhibited loss of fenestrations, increased EC thickening (vertical bar), and the appearance of multiple caveolae (arrows). (B) Quantification of the number of fenestrations per 1 µm revealed no significant change between Ad-null (3.6 ± 0.37; $n = 5$), Ad-sFlt1 (3.22 ± 0.2; $n = 3$), and (Ad-sEng (3.53 ± 0.43; $n = 5$), whereas only 1.17 ± 0.41 ($P < 0.05$; $n = 6$) were present in Ad-sFlt1 + Ad-sEng–treated mice CP. (C) Electron microscopic visualization of the ependymal cells in all experimental groups revealed normal apical polarity of the mitochondria (labeled M). Dashed lines indicate the cell–microvilli border, arrows indicate microvilli, and arrowheads indicate cilia. Bars: (A) 1.25 µm; (C) 2.5 µm.

in contrast intensity (day 8, 1.12 for Ad-sFlt1 + Ad-sEng vs. 1.02 for Ad-null [$P < 0.001$; $n = 6$]; and day 16, 1.17 for Ad-sFlt1 + Ad-sEng vs. 1.01 for Ad-null [$P < 0.0001$; $n = 7$]; Fig. 4 D).

Because RPLS has also been reported in association with bevacizumab treatment (24, 25), mice expressing Ad-sFlt1 or Ad-null for 28 d were imaged with MRI. There were no brain changes in mice expressing Ad-sFlt1 at days 8 or 16;

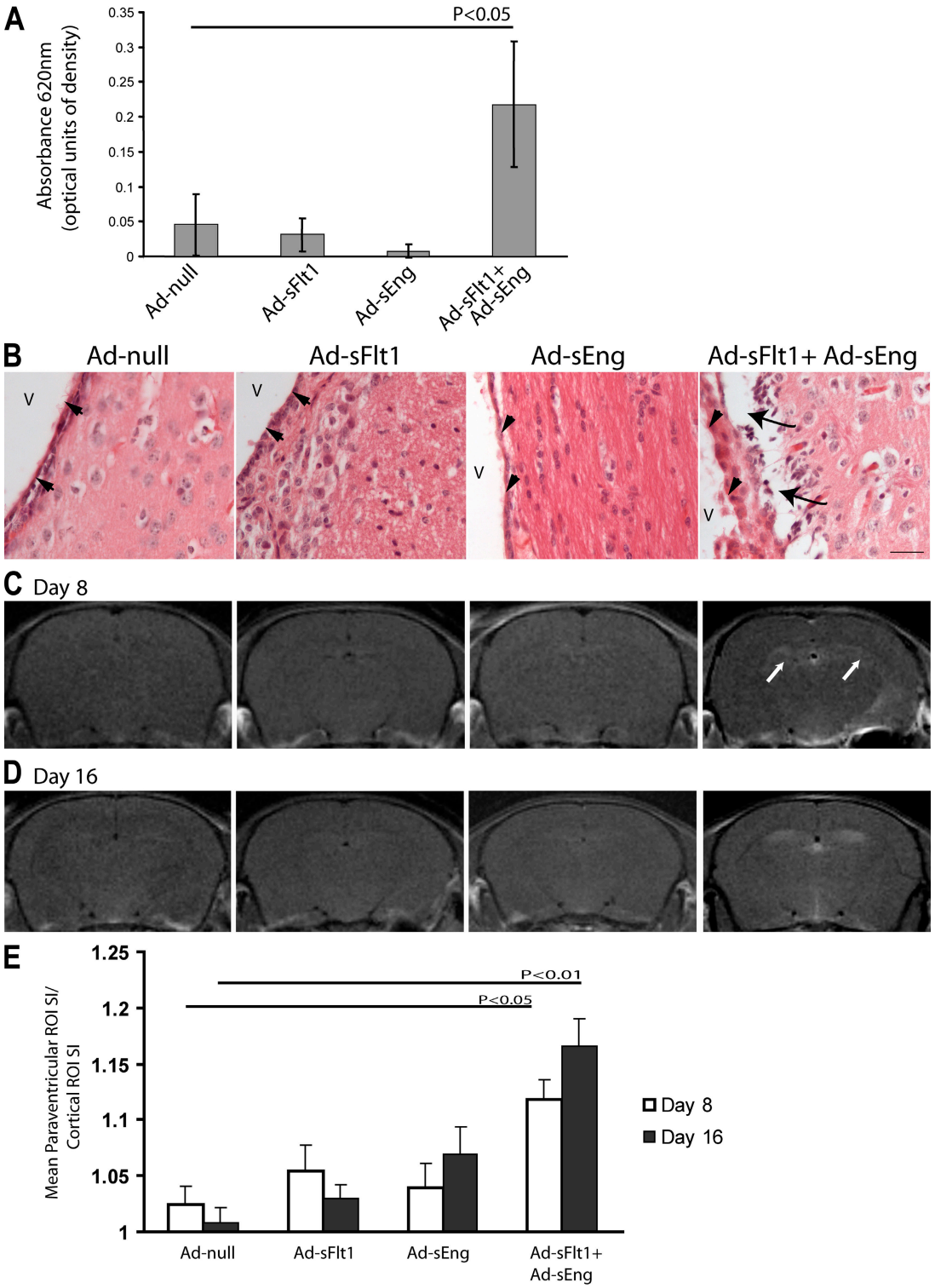

Figure 4. Effect of VEGF and TGF-β neutralization on brain permeability. (A) Experimental mice infected for 3 d were injected intravenously with 2% Evans blue in PBS. After 40 min, the brains were removed and quantified for Evans blue/albumin leakage. Simultaneous treatment with sFlt1 + sEng ($n = 3$) resulted in significantly increased Evans blue leakage into the extravascular space, whereas no changes could be detected with sFlt1 or sEng alone. Values represent means ± SD. (B) H + E staining of sections of the lateral ventricle of mice expressing sFlt1 + sEng for 14 d revealed marked periventricular edema (arrows) below the ependyma (arrowheads); no edema was observed in this region in other experimental or control mice. V, ventricle. Bar, 25 μm. (C and D) T1-weighted coronal MRI of experimental mice intravenously injected with Gd at 8 (C) and 16 (D) d after infection revealed focal lesions surrounding the lateral ventricles in the midcortex of mice expressing sFlt1 + sEng (white arrows) but not in the other experimental groups. (E) Quantification of the ratio of signal intensity in the periventricular zone versus the nonenhancing region in the cortex using ImageJ software (NIH). Values represent means ± SEM.

however, significant periventricular lesions were detected after 28 d of VEGF neutralization (Ad-null, 1.062 [$n = 4$] vs. Ad-sFlt1, 1.135 [$n = 5$]; $P < 0.02$; Fig. 5 A, arrows; and quantified in Fig. 5 B), providing support that extended VEGF blockade may result in RPLS. These mice displayed only a modest increase in mean arterial blood pressure at day 7 (Fig. 5 C).

DISCUSSION

We used Ad's expressing soluble receptors for VEGF (sFlt1) and TGF-β1 and TGF-β3 (sEng) to determine the effects of VEGF and TGF-β neutralization in adult mice. Immunohistochemical analysis and RT-PCR revealed expression of both VEGFR2 and TGF-βR2 in the CP, as well as on the ependymal cells that line the ventricles. The presence of both ligands and receptors implies a role for these growth factors in the CP and ependyma.

Neutralization of VEGF in adult mice for 14 d resulted in decreased perfusion of the CP vasculature associated with microthrombosis. The simultaneous neutralization of TGF-β did not lead to an increase in capillary nonperfusion over the time period examined. The loss CP vascular fenestrations of ependymal cell microvilli in mice expressing sFlt1 + sEng for 14 d implies that VEGF and TGF-β are similarly required for the maintenance of this cellular specialization. Permeability studies revealed periventricular focal lesions in mice in which VEGF and TGF-β were neutralized for 8 or 16 d, as well as in mice in which VEGF was neutralized for 28 d, suggesting that growth factor neutralization is sufficient to disrupt ventricular barrier function.

The role of TGF-β signaling in angiogenesis is context dependent, with reported actions both as a pro- and antiangiogenic stimulus (39, 40). Cultured ECs treated with TGF-β are typically growth arrested. Expression of Eng by ECs is greatly increased during angiogenesis and in multiple tumors (41). Mutations in Eng or the EC-specific TGF-β receptor TGF-βRI (activin receptor–like kinase 1) cause hereditary hemorrhagic telangiectasia 1 and 2, respectively, which are characterized by vascular malformations, suggesting a role for TGF-β signaling in vascular formation and/or stabilization.

Observations from this study add to the growing body of evidence that VEGF is critical to vessel stability and that neutralization may lead to microvascular damage (12, 21, 35, 42, 43). Disrupted vascular perfusion and fibrin accumulation in the CP is reminiscent of the cerebral changes noted in preeclampsia (44). Although VEGF neutralization is also associated with thrombosis in bevacizumab-treated patients (18), the mechanism is not known. Thrombosis may be initiated by the injury or activation of the endothelium and/or by a change in the balance of pro- and antithrombotic factors. We did not detect activated P-selectin or αIIbβIII on the platelets of mice expressing sFlt1 (unpublished data); thus, platelet activation is unlikely to be the basis of the observed thrombosis.

We observed that VEGF and TGF-β neutralization led to the loss of CP vessel fenestrations. Fenestrations are pore-like endothelial specializations, which may be diaphragmmed or nondiaphragmmed (45). Although decreased fenestrations have been reported in the kidney after VEGF neutralization (12, 43) and in the choriocapillaris following intravitreal bevacizumab treatment after 4 d (11), we only observed a minimal loss of fenestrations in the CP following systemic VEGF neutralization after 7 d, in contrast to a near complete loss of CP fenestrations in animals treated with sFlt1 + sEng. Plasmalemmal vesicle–associated protein has been shown to be associated with diaphragmmed fenestrae (46) and to be up-regulated by VEGF (47). Although high PV-1 levels are found in several fenestrated vascular beds, PV-1 is not detectable in whole brain extracts (46). Consistent with this observation, we did not detect PV-1 in the CP (unpublished data). We speculate that although VEGF has been shown to induce fenestrations in cultured ECs (10, 48), fenestrations lacking PV-1, such as those found in the CP, may be determined by both VEGF and TGF-β signaling.

After inhibition of TGF-β1 or VEGF, we observed decreased antiapoptotic *Bcl-x_L* expression, whereas combined TGF-β1/VEGF inhibition decreased both *Bcl-2* and *Bcl-x_L* expression. No change was detected in the proapoptotic markers *bax* or *bad*. Because antiapoptotic Bcl-2 proteins often function by binding proapoptotic Bcl-2 family members, a decrease in a single Bcl-2 family member is sufficient to trigger apoptosis (49, 50). Our findings suggest that both VEGF and TGF-β enhance survival through the Bcl-2 family genes.

Our results reveal ependymal cells as novel targets for VEGF and TGF-β. Ependymal microvilli are central to maintaining homeostasis and the transport of cerebrospinal fluid (CSF) through the ventricles (51); furthermore, enzymes localized to the microvilli mediate signaling and transport of molecules between the CSF and ependyma (52). Ependymal cells express TGF-βR2 during development (53), but the action of TGF-β on these cells in the adult has not been reported. A previous study of VEGFR2 on ependymal cells in vivo proposed that paracrine signaling of VEGF on ependymal cells is important for stimulation of adult neural stem cells and neurogenesis (54). We extend this observation by demonstrating that CP epithelial cells predominantly express the soluble VEGF120 isoform, which is presumably secreted into the CSF, as VEGF is detectable in normal CSF (54). As simultaneous neutralization of TGF-β and VEGF led to a loss of microvilli on the ependymal cells but did not affect perfusion of periventricular blood vessels (unpublished data), it seems likely that disruption of the ependymal barrier altered the homeostasis of the surrounding tissue, leading to loss of periventricular vasculature barrier function (55).

RPLS has been reported in some bevacizumab-treated patients and has been associated with primary vascular disorders such as eclampsia, thrombotic thrombocytopenic purpura, and cyclosporine toxicity (56). VEGF neutralization for 28 d, or VEGF and TGF-β1 neutralization for 8 or 16 d led to the development of similar focal lesions. RPLS has been speculated to be secondary to factors such as hypertension (23). Although blood pressure was elevated at day 7 in mice expressing sFlt1 + sEng (Fig. 5 C), the increase was modest, making it a less likely cause of the observed MRI lesions. Furthermore, although sEng expression resulted in an increase in blood

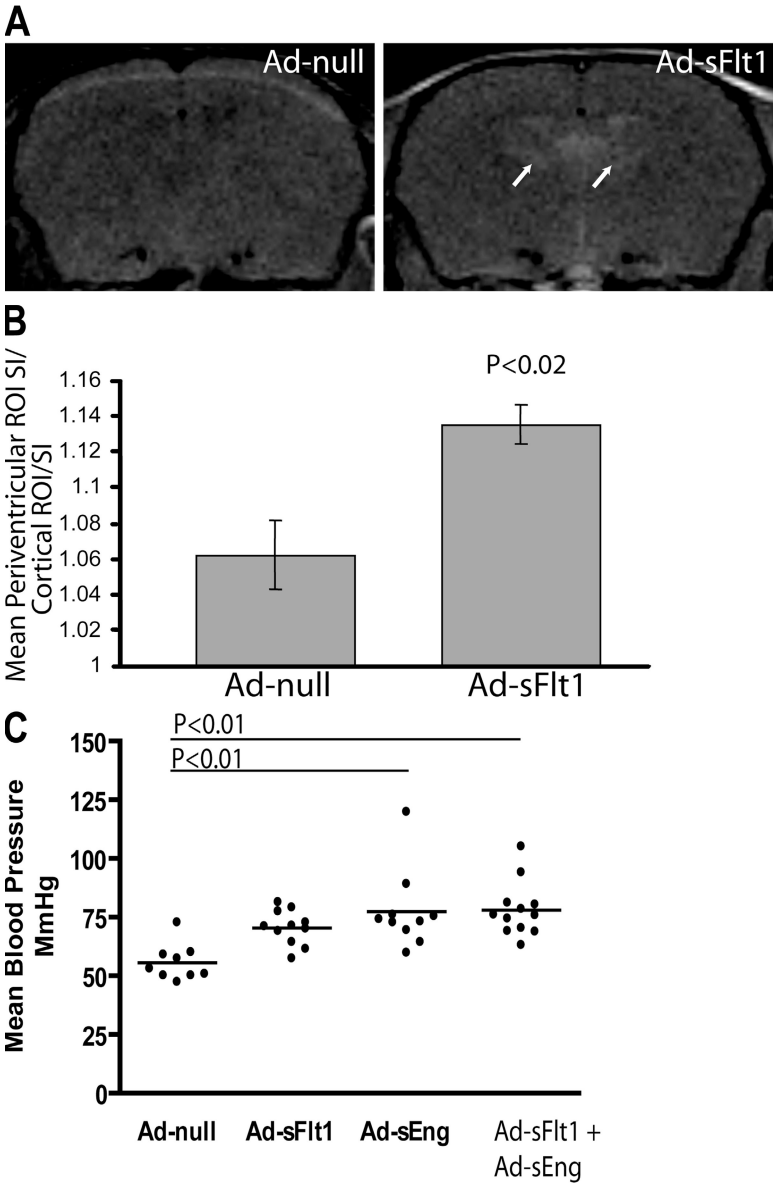

Figure 5. Effect of long-term VEGF neutralization on brain permeability, and effects of VEGF and TGF-β neutralization on blood pressure. (A and B) T1-weighted coronal MRI of Gd intravenously injected mice after 28 d of Ad-sFlt1 or Ad-null expression revealed focal lesions surrounding the lateral ventricles of significant intensity in the midcortex in Ad-sFlt1 mice. Areas in A represent the area of periventricular leakage observed on MRI. Values in B represent means ± SEM. (C) Noninvasive blood pressure measurement of experimental mice at day 7 Ad expression shows a small difference between Ad-null and Ad-sFlt1 mice but a significant difference between mice expressing Ad-null and Ad-sEng ($P < 0.01$) and Ad-sFlt1 + Ad-sEng ($P < 0.01$). Horizontal bars represent the average of the mean arterial pressure in the different groups.

pressure comparable to that noted with sFlt1 + sEng expression, no lesions were observed in these mice. Similarly, markers of endothelial damage, but not blood pressure, appear to correlate with brain edema in patients with preeclampsia/eclampsia who present with RPLS (56). Whether the focal lesions are reversible after cessation of VEGF and TGF-β neutralization remains to be explored.

High circulating levels of sFlt1 and sEng in the serum of preeclamptic patients appear responsible for many of the associated symptoms. Our data suggest that blockade of VEGF and TGF-β signaling results in disruption of the CP, which may lead to altered CSF dynamics and composition. In addition, ependymal cell dysfunction appears to result in disruption of ventricular barrier function and altered periventricular homeostasis, which may lead to the neurological manifestations observed in preeclampsia/eclampsia, including seizures.

Because the CP is the source of CSF, defects in the CP are likely to influence CSF production and composition. Observations of increased hemoglobin (57), protein (58), and α hydroxybutyric dehydrogenase (59) in the CSF of severely

preeclamptic patients supports this hypothesis. CP function may also contribute to Alzheimer's disease, amyotrophic lateral sclerosis, and other diseases of the CNS (60, 61), and the finding that both VEGF and TGF-β are altered in these diseases is consistent with their role in the integrity of the CP and ependyma.

MATERIALS AND METHODS

Mice. Mice used included adult *VEGF-lacZ* mice (62) for localization of VEGF expression, adult C57B6/J mice for RNA and for permeability experiments, and CD-1 mice. Animal protocols were approved by the Schepens Eye Research Institute and Beth Israel Deaconess Medical Center Institutional Animal Care and Use Committees.

Mice were injected via the tail vein with Ad's expressing sFlt1 (Ad-sFlt1), sEng (Ad-sEng), or empty Ad (Ad-null) as follows: 10^{10} viral particles (VP) for Ad-CMV-null (control), 2.5×10^9 VP for Ad-CMV-sFlt1, 7.5×10^9 VP for Ad-CMV-sEng, or 2.5×10^9 VP for Ad-CMV-sFlt1 plus 7.5×10^9 VP for Ad-CMV-sEng (Qbiogene) (32). Blood pressure was recorded on days 7 and 14 by volume pressure recording using a noninvasive blood pressure system (CODA 6; Kent Scientific) under 2% isoflurane anesthesia. sFlt1 and sEng plasma levels were determined by ELISA.

Fluorescein perfusion. After 14 d of Ad infection, mice were perfused over 2 min with 7 ml of 50 mg/ml of 2×10^6 mol wt fluorescein dextran in 4% paraformaldehyde via a 21-gauge cannula inserted into the aorta via the left ventricle, allowing fluid to exit via the right atrium.

Immunohistochemistry. Cryosections were cut at 10 μm and paraffin sections were cut at 6 μm. Sections were incubated overnight at 4°C with the following primary antibodies: rabbit polyclonal anti–coll IV (1:400; Abcam), rat monoclonal anti-CD31 (platelet/EC adhesion molecule 1; 1:100; clone MEC 13.3; BD Biosciences), rabbit polyclonal antifibrinogen (1:250; Dako) (36), rabbit anti–mouse VEGFR2-T1014 (1:500; a gift from R. Brekken, University of Texas Southwestern Medical Center, Dallas, TX), and rabbit polyclonal anti–mouse TGF-βR2 (1:100; Santa Cruz Biotechnology, Inc.) diluted in blocking solution (0.2% Tween, 3% donkey serum, 3% goat serum). Secondary antibodies included cyanine 3–donkey anti–rabbit (Jackson ImmunoResearch Laboratories) with nuclear TO-PRO-3 iodide stain (Invitrogen) and biotin-conjugated anti–rabbit (Vector Laboratories). Antibodies were visualized with avidin-biotin peroxidase and 3-amino-9-ethylcarbazole (AEC) or 3,3′-diaminobenzidine (DAB) substrates (ABC kit; Vector Laboratories). For *VEGF-lacZ*, slides were first stained for LacZ using the in situ β-galactosidase kit (Stratagene).

TEM. After 14 d of infection with Ad, mice were perfused as described in fluorescein perfusion using 10 ml of sodium cacodylate buffer (0.2 M, pH 7.4), followed by 10 ml of half-strength Karnovsky's fixative. The third and fourth ventricles were dissected and fixed with half-strength Karnovsky's fixative, followed by 2% osmium tetroxide and en block stain with 0.5% uranyl acetate. After dehydration and embedding, ultra-thin sections were visualized using a transmission electron microscope (model 410; Phillips).

RNA isolation and PCR. CP from the lateral third and fourth ventricles were dissected and pooled from four mice for RNA extraction using the RNAqueous-4PCR kit (Ambion). RNA was reverse transcribed using Superscript II (Invitrogen; Table I).

For quantification of VEGF isoform expression, standard curves were generated and normalized to 18S using a sequence detection system (Prism 9700; Applied Biosystems). For pro- and antiapoptotic genes, data were analyzed by the comparative threshold cycle method using GAPDH as an endogenous control.

Vascular permeability. Vascular permeability was assessed using Evans blue, as previously described (32). After 72 h, mice were anesthetized and injected retroorbitally with 2% Evans blue dye. 40 min later, mice were perfused with PBS containing 2 mM EDTA for 20 min. Brains were harvested and incubated in formamide at 70°C for 24 h Supernatants containing extravascular Evans blue were collected after centrifugation at 14,000 rpm for 10 min. The OD was measured at 620 nm and was corrected for contamination with heme pigments using the formula OD_{620} (corrected) = $OD_{620} - (1.326 \times OD_{740} + 0.03)$.

For quantification of endothelial fenestrations, segments of individual capillaries were photographed at a final magnification of 10,400 (one vessel from three to six animals per group). Fenestrations were quantified per 1 μm, and data represent the mean of three segments (±SEM) of three to six vessels per group.

Table I. Mouse primers used in RT-PCR and real-time PCR

Transcript	Primer	Sequence	Reference
VEGFR2	5′	5′-GCCCTGCTGTGGTCTCACTAC-3′	reference 64
	3′	5′-CAAAGCATTGCCCATTCGAT-3′	
TGF-β1	5′	5′-GCTGCGCTTGCAGAGATTAAA-3′	reference 65
	3′	5′-TTGCTGTACTGTGTGTCCAG-3′	
TGF-βRII	5′	5′-CGTGTGGAGGAAGAACAACA-3′	reference 65
	3′	5′-TCTCAAACTGCTCTGAGGTG-3′	
VEGF common forward	5′	5′-GCCAGCACATAGAGAGAATGAGC-3′	reference 13
VEGF 120 reverse	3′	5′-CGGCTTGTCACATTTTTCTGG-3′	reference 13
VEGF 164 reverse	3′	5′-CAAGGCTCACAGTGATTTTCTGG-3′	reference 13
VEGF 188 reverse	3′	5′-AACAAGGCTCACAGTGAACGC T-3′	reference 13
Bax	5′	5′-AAGCTGAGCGAGTGTCTCCGGCG-3′	reference 66
	3′	5′-GCCACAAAGATGGTCACTGTCTGCC-3′	
Bad	5′	5′-CCAGTGATCTTCTGCTCCACATCCC-3′	reference 66
	3′	5′-CAACTTAGCACAGGCACCCGAGGG-3′	
Bcl-2	5′	5′-CTCGTCGCTACCGTCGTGACTTCG-3′	reference 66
	3′	5′-CAGATGCCGGTTCAGGTACTCAGTC-3′	
Bcl-x_L	5′	5′-TGGAGTAAACTGGGGGTCGCATCG-3′	reference 66
	3′	5′-AGCCACCGTCATGCCCGTCAGG-3′	
GAPDH	5′	5′-GTGCAAAGTGGAGATGGTGCC-3′	reference 67
	3′	5′-GATGATGACCCGTTTGGCTCC-3′	

MRI. MRI was performed at days 8, 16, and 28 after infection. Mice were positioned inside the magnet immediately after intravenous injection of 0.3 mmol Gd/kg (Magnevist; Schering AG). Magnetic resonance images were acquired with a 4.7-tesla magnet using a transmit-receive, birdcage, volume coil with an inner diameter of 35 mm (Bruker BioSpin). T2-weighted images were acquired covering the entire brain using a fast spin echo sequence with the following parameters: recovery time (TR) = 1000 ms, echo time (TE) = 6.6 ms, echo train = 8, field of view (FOV) = 30 × 30 mm^2, matrix = 128 × 128, slice thickness = 1 mm (gapless), slice orientation = ventrocaudal plane, and number of slices = 15 (covering the entire brain). A T1-weighted sequence was conducted with identical geometry as described for the T2-weighted sequence and the following parameters: TR = 500 ms, TE = 11 ms, and number of excitations = 4. The T1- and T2-weighted sequences yielded an in-plane resolution of 234 × 234 mm^2.

Statistical analysis. Data were analyzed by the unpaired Student's *t* test. $P < 0.05$ was significant, and means ± SEM are presented. For the Evans blue extravasation experiment, data are represented as the mean ± SD.

We thank Dr. Scott Plotkin for analysis of the MRI, Mrs. Patricia Pearson for assistance with TEM, and Mrs. Christine Bagley and Miss Knatokie Ford for their critical review of the manuscript.

This work was supported by National Institutes of Health (NIH) grants EY05318, EY015435, and CA45548; Research to Prevent Blindness; a Senior Scientific Investigator Award to P.A. D'Amore; and NIH grants DK065997 and HL079594 to S.A. Karumanchi. A.S.R. Maharaj was supported by National Institute of General Medical Sciences predoctoral fellowship NIH-F31-GM65079. P.A. D'Amore is a Research to Prevent Blindness Senior Scientific Investigator.

S.A. Karumanchi is a co-inventor on provisional patents filed by the Beth Israel Deaconess Medical Center for the diagnosis and therapy of preeclampsia and is a consultant to Abbott Diagnostics, Beckman Coulter, and Johnson & Johnson. All other authors declare no conflicting financial interests.

Submitted: 20 September 2007
Accepted: 16 January 2008

REFERENCES

1. Coultas, L., K. Chawengsaksophak, and J. Rossant. 2005. Endothelial cells and VEGF in vascular development. *Nature*. 438:937–945.
2. Carmeliet, P., V. Ferreira, G. Breier, S. Pollefeyt, L. Kieckens, M. Gertsenstein, M. Fahrig, A. Vandenhoeck, K. Harpal, C. Eberhardt, et al. 1996. Abnormal blood vessel development and lethality in embryos lacking a single VEGF allele. *Nature*. 380:435–439.
3. Ferrara, N., K. Carver-Moore, H. Chen, M. Dowd, L. Lu, K.S. O'Shea, L. Powell-Braxton, K.J. Hillan, and M.W. Moore. 1996. Heterozygous embryonic lethality induced by targeted inactivation of the VEGF gene. *Nature*. 380:439–442.
4. Miquerol, L., B.L. Langille, and A. Nagy. 2000. Embryonic development is disrupted by modest increases in vascular endothelial growth factor gene expression. *Development*. 127:3941–3946.
5. Eming, S.A., and T. Krieg. 2006. Molecular mechanisms of VEGF-A action during tissue repair. *J. Investig. Dermatol. Symp. Proc.* 11:79–86.
6. Otani, N., S. Minami, M. Yamoto, T. Shikone, H. Otani, R. Nishiyama, T. Otani, and R. Nakano. 1999. The vascular endothelial growth factor/fms-like tyrosine kinase system in human ovary during the menstrual cycle and early pregnancy. *J. Clin. Endocrinol. Metab.* 84:3845–3851.
7. Adamis, A.P., and D.T. Shima. 2005. The role of vascular endothelial growth factor in ocular health and disease. *Retina*. 25:111–118.
8. Folkman, J. 1995. Angiogenesis in cancer, vascular, rheumatoid and other disease. *Nat. Med.* 1:27–31.
9. Darland, D.C., L.J. Massingham, S.R. Smith, E. Piek, M. Saint-Geniez, and P.A. D'Amore. 2003. Pericyte production of cell-associated VEGF is differentiation-dependent and is associated with endothelial survival. *Dev. Biol.* 264:275–288.
10. Esser, S., K. Wolburg, H. Wolburg, G. Breier, T. Kurzchalia, and W. Risau. 1998. Vascular endothelial growth factor induces endothelial fenestrations in vitro. *J. Cell Biol.* 140:947–959.
11. Peters, S., P. Heiduschka, S. Julien, F. Ziemssen, H. Fietz, K.U. Bartz-Schmidt, and U. Schraermeyer. 2007. Ultrastructural findings in the primate eye after intravitreal injection of bevacizumab. *Am. J. Ophthalmol.* 143:995–1002.
12. Kamba, T., B.Y. Tam, H. Hashizume, A. Haskell, B. Sennino, M.R. Mancuso, S.M. Norberg, S.M. O'Brien, R.B. Davis, L.C. Gowen, et al. 2006. VEGF-dependent plasticity of fenestrated capillaries in the normal adult microvasculature. *Am. J. Physiol. Heart Circ. Physiol.* 290:H560–H576.
13. Saint-Geniez, M., A.E. Maldonado, and P.A. D'Amore. 2006. VEGF expression and receptor activation in the choroid during development and in the adult. *Invest. Ophthalmol. Vis. Sci.* 47:3135–3142.
14. Maharaj, A.S., M. Saint-Geniez, A.E. Maldonado, and P.A. D'Amore. 2006. Vascular endothelial growth factor localization in the adult. *Am. J. Pathol.* 168:639–648.
15. Maharaj, A.S., and P.A. D'Amore. 2007. Roles for VEGF in the adult. *Microvasc. Res.* 74:100–113.
16. D'Amore, P.A. 2007. Vascular endothelial cell growth factor-a: not just for endothelial cells anymore. *Am. J. Pathol.* 171:14–18.
17. Hurwitz, H., L. Fehrenbacher, W. Novotny, T. Cartwright, J. Hainsworth, W. Heim, J. Berlin, A. Baron, S. Griffing, E. Holmgren, et al. 2004. Bevacizumab plus irinotecan, fluorouracil, and leucovorin for metastatic colorectal cancer. *N. Engl. J. Med.* 350:2335–2342.
18. Hurwitz, H., and S. Saini. 2006. Bevacizumab in the treatment of metastatic colorectal cancer: safety profile and management of adverse events. *Semin. Oncol.* 33:S26–S34.
19. Sandler, A., R. Gray, M.C. Perry, J. Brahmer, J.H. Schiller, A. Dowlati, R. Lilenbaum, and D.H. Johnson. 2006. Paclitaxel-carboplatin alone or with bevacizumab for non-small-cell lung cancer. *N. Engl. J. Med.* 355:2542–2550.
20. Sibai, B., G. Dekker, and M. Kupferminc. 2005. Pre-eclampsia. *Lancet*. 365:785–799.
21. Maynard, S.E., J.Y. Min, J. Merchan, K.H. Lim, J. Li, S. Mondal, T.A. Libermann, J.P. Morgan, F.W. Sellke, I.E. Stillman, et al. 2003. Excess placental soluble fms-like tyrosine kinase 1 (sFlt1) may contribute to endothelial dysfunction, hypertension, and proteinuria in preeclampsia. *J. Clin. Invest.* 111:649–658.
22. Yang, J.C., L. Haworth, R.M. Sherry, P. Hwu, D.J. Schwartzentruber, S.L. Topalian, S.M. Steinberg, H.X. Chen, and S.A. Rosenberg. 2003. A randomized trial of bevacizumab, an anti-vascular endothelial growth factor antibody, for metastatic renal cancer. *N. Engl. J. Med.* 349:427–434.
23. Hinchey, J., C. Chaves, B. Appignani, J. Breen, L. Pao, A. Wang, M.S. Pessin, C. Lamy, J.L. Mas, and L.R. Caplan. 1996. A reversible posterior leukoencephalopathy syndrome. *N. Engl. J. Med.* 334:494–500.
24. Glusker, P., L. Recht, and B. Lane. 2006. Reversible posterior leukoencephalopathy syndrome and bevacizumab. *N. Engl. J. Med.* 354:980–982.
25. Ozcan, C., S.J. Wong, and P. Hari. 2006. Reversible posterior leukoencephalopathy syndrome and bevacizumab. *N. Engl. J. Med.* 354:980–982.
26. Loureiro, R.M., and P.A. D'Amore. 2005. Transcriptional regulation of vascular endothelial growth factor in cancer. *Cytokine Growth Factor Rev.* 16:77–89.
27. Orlidge, A., and P.A. D'Amore. 1987. Inhibition of capillary endothelial cell growth by pericytes and smooth muscle cells. *J. Cell Biol.* 105:1455–1462.
28. Sato, Y., and D.B. Rifkin. 1989. Inhibition of endothelial cell movement by pericytes and smooth muscle cells: activation of a latent transforming growth factor-beta 1–like molecule by plasmin during co-culture. *J. Cell Biol.* 109:309–315.
29. Bian, Z.M., S.G. Elner, and V.M. Elner. 2007. Regulation of VEGF mRNA expression and protein secretion by TGF-beta2 in human retinal pigment epithelial cells. *Exp. Eye Res.* 84:812–822.
30. Jeon, S.H., B.C. Chae, H.A. Kim, G.Y. Seo, D.W. Seo, G.T. Chun, N.S. Kim, S.W. Yie, W.H. Byeon, S.H. Eom, et al. 2007. Mechanisms underlying TGF-beta1-induced expression of VEGF and Flk-1 in mouse macrophages and their implications for angiogenesis. *J. Leukoc. Biol.* 81:557–566.
31. Tokuda, H., D. Hatakeyama, S. Akamatsu, K. Tanabe, M. Yoshida, T. Shibata, and O. Kozawa. 2003. Involvement of MAP kinases in TGF-beta-stimulated vascular endothelial growth factor synthesis in osteoblasts. *Arch. Biochem. Biophys.* 415:117–125.

32. Venkatesha, S., M. Toporsian, C. Lam, J. Hanai, T. Mammoto, Y.M. Kim, Y. Bdolah, K.H. Lim, H.T. Yuan, T.A. Libermann, et al. 2006. Soluble endoglin contributes to the pathogenesis of preeclampsia. *Nat. Med.* 12:642–649.
33. Levine, R.J., C. Lam, C. Qian, K.F. Yu, S.E. Maynard, B.P. Sachs, B.M. Sibai, F.H. Epstein, R. Romero, R. Thadhani, and S.A. Karumanchi. 2006. Soluble endoglin and other circulating antiangiogenic factors in preeclampsia. *N. Engl. J. Med.* 355:992–1005.
34. Flood, C., J. Akinwunmi, C. Lagord, M. Daniel, M. Berry, A. Jackowski, and A. Logan. 2001. Transforming growth factor-beta1 in the cerebrospinal fluid of patients with subarachnoid hemorrhage: titers derived from exogenous and endogenous sources. *J. Cereb. Blood Flow Metab.* 21:157–162.
35. Inai, T., M. Mancuso, H. Hashizume, F. Baffert, A. Haskell, P. Baluk, D.D. Hu-Lowe, D.R. Shalinsky, G. Thurston, G.D. Yancopoulos, and D.M. McDonald. 2004. Inhibition of vascular endothelial growth factor (VEGF) signaling in cancer causes loss of endothelial fenestrations, regression of tumor vessels, and appearance of basement membrane ghosts. *Am. J. Pathol.* 165:35–52.
36. Baffert, F., T. Le, B. Sennino, G. Thurston, C.J. Kuo, D. Hu-Lowe, and D.M. McDonald. 2006. Cellular changes in normal blood capillaries undergoing regression after inhibition of VEGF signaling. *Am. J. Physiol. Heart Circ. Physiol.* 290:H547–H559.
37. Gupta, S. 2003. Molecular signaling in death receptor and mitochondrial pathways of apoptosis. *Int. J. Oncol.* 22:15–20.
38. Runge, V.M., L.R. Muroff, and J.W. Wells. 1997. Principles of contrast enhancement in the evaluation of brain diseases: an overview. *J. Magn. Reson. Imaging.* 7:5–13.
39. Mallet, C., D. Vittet, J.J. Feige, and S. Bailly. 2006. TGFbeta1 induces vasculogenesis and inhibits angiogenic sprouting in an embryonic stem cell differentiation model: respective contribution of ALK1 and ALK5. *Stem Cells.* 24:2420–2427.
40. Lebrin, F., M.J. Goumans, L. Jonker, R.L. Carvalho, G. Valdimarsdottir, M. Thorikay, C. Mummery, H.M. Arthur, and P. ten Dijke. 2004. Endoglin promotes endothelial cell proliferation and TGF-beta/ALK1 signal transduction. *EMBO J.* 23:4018–4028.
41. Burrows, F.J., E.J. Derbyshire, P.L. Tazzari, P. Amlot, A.F. Gazdar, S.W. King, M. Letarte, E.S. Vitetta, and P.E. Thorpe. 1995. Up-regulation of endoglin on vascular endothelial cells in human solid tumors: implications for diagnosis and therapy. *Clin. Cancer Res.* 1:1623–1634.
42. Gerber, H.P., X. Wu, L. Yu, C. Wiesmann, X.H. Liang, C.V. Lee, G. Fuh, C. Olsson, L. Damico, D. Xie, et al. 2007. Mice expressing a humanized form of VEGF-A may provide insights into the safety and efficacy of anti-VEGF antibodies. *Proc. Natl. Acad. Sci. USA.* 104:3478–3483.
43. Eremina, V., M. Sood, J. Haigh, A. Nagy, G. Lajoie, N. Ferrara, H.P. Gerber, Y. Kikkawa, J.H. Miner, and S.E. Quaggin. 2003. Glomerular-specific alterations of VEGF-A expression lead to distinct congenital and acquired renal diseases. *J. Clin. Invest.* 111:707–716.
44. Hansen, W.F., S.J. Burnham, T.O. Svendsen, V.L. Katz, J.M. Thorp Jr., and A.R. Hansen. 1996. Transcranial Doppler findings of cerebral vasospasm in preeclampsia. *J. Matern. Fetal Med.* 5:194–200.
45. Bates, D.O., N.J. Hillman, B. Williams, C.R. Neal, and T.M. Pocock. 2002. Regulation of microvascular permeability by vascular endothelial growth factors. *J. Anat.* 200:581–597.
46. Stan, R.V., M. Kubitza, and G.E. Palade. 1999. PV-1 is a component of the fenestral and stomatal diaphragms in fenestrated endothelia. *Proc. Natl. Acad. Sci. USA.* 96:13203–13207.
47. Strickland, L.A., A.M. Jubb, J.A. Hongo, F. Zhong, J. Burwick, L. Fu, G.D. Frantz, and H. Koeppen. 2005. Plasmalemmal vesicle-associated protein (PLVAP) is expressed by tumour endothelium and is upregulated by vascular endothelial growth factor-A (VEGF). *J. Pathol.* 206:466–475.
48. Satchell, S.C., C.H. Tasman, A. Singh, L. Ni, J. Geelen, C.J. von Ruhland, M.J. O'Hare, M.A. Saleem, L.P. van den Heuvel, and P.W. Mathieson. 2006. Conditionally immortalized human glomerular endothelial cells expressing fenestrations in response to VEGF. *Kidney Int.* 69:1633–1640.
49. Kim, H.S., K.K. Hwang, J.W. Seo, S.Y. Kim, B.H. Oh, M.M. Lee, and Y.B. Park. 2000. Apoptosis and regulation of Bax and Bcl-X proteins during human neonatal vascular remodeling. *Arterioscler. Thromb. Vasc. Biol.* 20:957–963.
50. Yamamoto, K., R. Morishita, S. Hayashi, H. Matsushita, H. Nakagami, A. Moriguchi, K. Matsumoto, T. Nakamura, Y. Kaneda, and T. Ogihara. 2001. Contribution of Bcl-2, but not Bcl-xL and Bax, to antiapoptotic actions of hepatocyte growth factor in hypoxia-conditioned human endothelial cells. *Hypertension.* 37:1341–1348.
51. Del Bigio, M.R. 1995. The ependyma: a protective barrier between brain and cerebrospinal fluid. *Glia.* 14:1–13.
52. Ogawa, M., M. Shiozawa, Y. Hiraoka, Y. Takeuchi, and S. Aiso. 1998. Immunohistochemical study of localization of gamma-glutamyl transpeptidase in the rat brain. *Tissue Cell.* 30:597–601.
53. Lawler, S., A.F. Candia, R. Ebner, L. Shum, A.R. Lopez, H.L. Moses, C.V. Wright, and R. Derynck. 1994. The murine type II TGF-beta receptor has a coincident embryonic expression and binding preference for TGF-beta 1. *Development.* 120:165–175.
54. Schanzer, A., F.P. Wachs, D. Wilhelm, T. Acker, C. Cooper-Kuhn, H. Beck, J. Winkler, L. Aigner, K.H. Plate, and H.G. Kuhn. 2004. Direct stimulation of adult neural stem cells in vitro and neurogenesis in vivo by vascular endothelial growth factor. *Brain Pathol.* 14:237–248.
55. Segal, M.B. 2000. The choroid plexuses and the barriers between the blood and the cerebrospinal fluid. *Cell. Mol. Neurobiol.* 20:183–196.
56. Schwartz, R.B., S.K. Feske, J.F. Polak, U. DeGirolami, A. Iaia, K.M. Beckner, S.M. Bravo, R.A. Klufas, R.Y. Chai, and J.T. Repke. 2000. Preeclampsia-eclampsia: clinical and neuroradiographic correlates and insights into the pathogenesis of hypertensive encephalopathy. *Radiology.* 217:371–376.
57. Norwitz, E.R., L.C. Tsen, J.S. Park, P.A. Fitzpatrick, D.M. Dorfman, G.R. Saade, C.S. Buhimschi, and I.A. Buhimschi. 2005. Discriminatory proteomic biomarker analysis identifies free hemoglobin in the cerebrospinal fluid of women with severe preeclampsia. *Am. J. Obstet. Gynecol.* 193:957–964.
58. Fish, S.A., J.C. Morrison, E.T. Bucovaz, W.L. Wiser, and W.D. Whybrew. 1972. Cerebral spinal fluid studies in eclampsia. *Am. J. Obstet. Gynecol.* 112:502–512.
59. Morrison, J.C., D.W. Whybrew, W.L. Wiser, E.T. Bucovaz, and S.A. Fish. 1971. Enzyme levels in the serum and cerebrospinal fluid in eclampsia. *Am. J. Obstet. Gynecol.* 110:619–624.
60. Lambrechts, D., E. Storkebaum, M. Morimoto, J. Del-Favero, F. Desmet, S.L. Marklund, S. Wyns, V. Thijs, J. Andersson, I. van Marion, et al. 2003. VEGF is a modifier of amyotrophic lateral sclerosis in mice and humans and protects motoneurons against ischemic death. *Nat. Genet.* 34:383–394.
61. Stopa, E.G., T.M. Berzin, S. Kim, P. Song, V. Kuo-LeBlanc, M. Rodriguez-Wolf, A. Baird, and C.E. Johanson. 2001. Human choroid plexus growth factors: What are the implications for CSF dynamics in Alzheimer's disease? *Exp. Neurol.* 167:40–47.
62. Miquerol, L., M. Gertsenstein, K. Harpal, J. Rossant, and A. Nagy. 1999. Multiple developmental roles of VEGF suggested by a LacZ-tagged allele. *Dev. Biol.* 212:307–322.
63. Mancuso, M.R., R. Davis, S.M. Norberg, S. O'Brien, B. Sennino, T. Nakahara, V.J. Yao, T. Inai, P. Brooks, B. Freimark, et al. 2006. Rapid vascular regrowth in tumors after reversal of VEGF inhibition. *J. Clin. Invest.* 116:2610–2621.
64. Shih, S.C., G.S. Robinson, C.A. Perruzzi, A. Calvo, K. Desai, J.E. Green, I.U. Ali, L.E. Smith, and D.R. Senger. 2002. Molecular profiling of angiogenesis markers. *Am. J. Pathol.* 161:35–41.
65. Watabe, T., A. Nishihara, K. Mishima, J. Yamashita, K. Shimizu, K. Miyazawa, S. Nishikawa, and K. Miyazono. 2003. TGF-β receptor kinase inhibitor enhances growth and integrity of embryonic stem cell–derived endothelial cells. *J. Cell Biol.* 163:1303–1311.
66. Jayanthi, S., X. Deng, M. Bordelon, M.T. McCoy, and J.L. Cadet. 2001. Methamphetamine causes differential regulation of pro-death and anti-death Bcl-2 genes in the mouse neocortex. *FASEB J.* 15:1745–1752.
67. Takabatake, T., M. Ogawa, T.C. Takahashi, M. Mizuno, M. Okamoto, and K. Takeshima. 1997. Hedgehog and patched gene expression in adult ocular tissues. *FEBS Lett.* 410:485–489.